

## PROPERTIES OF RARE EARTH Ga-La-S GLASSES OBTAINED BY RF INDUCTOR HEATING

A. A. POPESCU\*, D. SAVASTRU, S. MICLOS, V. BRAIC, M. POPESCU<sup>a</sup>,  
A. MANEA<sup>a</sup>, A. KISS

*National Institute of R&D for Optoelectronics INOE2000, 409 Atomistilor str.,  
Magurele, Ilfov, 077125, Romania*

*<sup>a</sup>National Institute of R&D for Materials Physics, 105 bis Atomistilor str.,  
Magurele, Ilfov, 077125, Romania*

A new synthesis method for  $70\text{Ga}_2\text{S}_330\text{La}_2\text{S}_3$  (GLS) lanthanum based glass, which uses a RF-heating inductor, has been developed. The method gives the possibility to quench the melt without taking the crucible out of the reaction chamber. Glasses with good optical quality were obtained. The samples characterized by X-ray diffraction prove the amorphous state. The re-heating of GaLaS at temperatures of 620 °C leads to the appearance of large 30-80  $\mu\text{m}$  crystals,  $\text{Ga}_3\text{La}_{1.66}\text{S}_7$  structure being the main crystal form. High quality GLS thin films have been obtained by RF sputtering. The calculated refractive index was 2.48 for the thin films obtained by RF sputtering and 2.55 for bulk samples. Two kinds of the Urbach-density of state distribution are distinguished from optical transmission measurements corresponding to activation energies of 0.12 eV and 0.66 eV.

(Received February 11, 2011; accepted February 28, 2011)

*Keywords:* Chalcogenide glasses; Rare-earth; Refractive index; Optical spectra

### 1. Introduction

For several years, non-crystalline As(Ge, Sb, Te) chalcogenide glasses have been investigated due to their multiple applications such as IR transparent and humidity-proof windows, optical recording media and even photoresist. The stability of these materials against strong laser radiation has yet been insufficiently proved. Lack of a sharp phase transition significantly lowers their softening temperature down to about 150-300 °C.

The chalcogenides of the rare earths elements based on lanthanum can be considered most promising. The synthesis of the most studied of them - gallium lanthanum sulphide (GaLaS) was first reported by Lozach et al in 1976 [1]. They have studied the phase diagram putting into evidence a quite large domain where glass state is obtained. Optimal conditions for vitrification occur around the composition  $70\text{Ga}_2\text{S}_330\text{La}_2\text{S}_3$  %mol (GLS).

The interest in GLS materials increased lately due to new potential applications in photonics as a host for rare-earth elements [2,3], fabrication of optical fibers [4,5] and active laser media with new laser transitions in the IR. Applications in nonlinear optics and nano-photonics are attractive due to large the Kerr-nonlinearity and refractive index [6,7] of these chalcogenides. Photonic crystal fabrication was successfully confirmed [8]. The pulsed laser deposition method for GLS amorphous thin films was investigated [9] and new possibilities of direct laser writing to create waveguide channels were demonstrated for GaLaS [10] and other chalcogenide materials[11]. New phenomena like the realization of photonic structure [12,13] may occur in this materials.

---

\*Corresponding author: apopescu@inoe.inoe.ro

There are two factors that make the bulk preparation still difficult: *i*) the high melting temperature of La and also of  $\text{La}_2\text{S}_3$  (about 2000 °C) and *ii*) the high chemical reactivity of GaLaS compounds at such high temperatures. The first difficulty can be overcome by adding a significant amount of  $\text{Ga}_2\text{S}_3$  (melting point 1050 °C), which produces an amalgam of  $\text{La}_3\text{S}_3$  whose melting temperature touches at about 1150 °C. Concerning the reactivity with the crucible, a solution may be the use of the graphite. However, since the glass preparation requires rather rapid quenching of melt and graphite flares at about 600 °C in air, it can't be used in a direct quenching process in air or water. A generally approved way is to use either a graphite crucible sealed in a silica tube or an open silica tube with a graphite crucible inside. Adequate quenching is not so predictable under such conditions. The basic idea of the present work is the use of the direct heating of an open graphite crucible using a RF coil. The mixture of  $\text{Ga}_2\text{S}_3/\text{La}_2\text{S}_3$  powder is heated up to a synthesis temperature of 1150 °C in pure Ar atmosphere. Preparation conditions and characterization of material properties are described.

## 2. Glass preparation

*Bulk synthesis:*  $\text{Ga}_2\text{S}_3/\text{La}_2\text{S}_3$  precursors of composition 70 $\text{Ga}_2\text{S}_3$  and 30 $\text{La}_2\text{S}_3$  %mol (GLS) are weighed directly in a glassy carbon crucible (ALFA AESAR). The crucible is then set as fast as possible inside the silica tube and purged with pure Ar gas.

The schematic setup of the preparation method is presented in Fig.1. The glassy carbon crucible (2) containing a mixture of  $\text{Ga}_2\text{S}_3/\text{La}_2\text{S}_3$  powder (1) is placed in a second graphite container (3), which is heated by absorbed electromagnetic radiation. A 150 kHz generator powers the inductor (7). The design of the graphite container plays an important role. The bottom of the container is drilled, offering an increased gas flow that will directly cool down the graphite crucible and quench the GLS melt. The side wall has a cutting which diminishes the screening of RF-field, so that the radiation is directly absorbed by the graphite crucible. Such design allows the equalization of the melting temperature and a high quenching rate. The ceramic screen (4) diminishes heat losses by radiation. A transparent fused silica tube (5) makes the reaction chamber. A rubber gasket (6) seals the chamber. A mechanical vacuum pump is used during the heating up to 600°C. Then pure Ar gas flows inside the chamber.

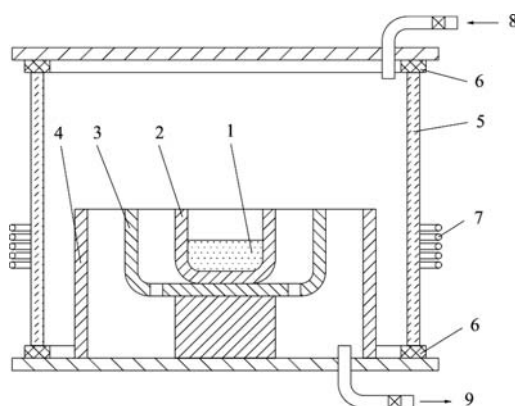


Fig. 1. Technological setup of GLS glass preparation: 1-  $\text{Ga}_2\text{S}_3/\text{La}_2\text{S}_3$  powder mixture; 2 - Glassy carbon crucible; 3 - Graphite container; 4 - Ceramic screen; 4 - Fused silica tube; 5 - Rubber sealing gasket; 7 - Radio frequency inductor; 8 - Ar gas inlet; 9 - Ar gas outlet

The temperature inside the crucible was calibrated as a function of applied RF power before the initialization of the synthesis process. The temperature of the mixture is slowly raised during 12 hours. The synthesis takes place three to six hours at 1150 °C. Quenching is assured by increasing the gas flow after RF power was disconnected.

Thin film deposition: The deposition enclosure was evacuated down to a pressure of  $2 \cdot 10^{-4}$  Pa. The BK7 glass samples were heated up to a temperature of 120 °C in order to eliminate the water vapors and cleaned by Ar ion bombardment. The GLS thin layers deposition was achieved using a cylindrical magnetron with a 1 inch diameter cathode. The magnetron was fed with a 13.56 MHz RF voltage at a power of 25 W. The Ar pressure during deposition was maintained at 0.8 Pa. The distance between target and the substrate holder was 112 mm. For a better adhesion of the film, the substrate temperature during deposition was held at 120 °C. After two hours of deposition, 220 nm thick transparent films were obtained.

### 3. Characterisation

The structure was investigated by X-ray diffraction (XRD) using a BRUKER D8 ADVANCE diffractometer in a divergent beam setting; Bragg-Brentano geometry with Lynx Eye detector, using a filtered Cu K $\alpha$  incident radiation. The optical transmission measurements were performed with Perkin Elmer Lambda 1050 and FTIR spectrophotometers. Standard AFM and optical images were obtained.

#### 3.1 Glass formation and properties

The material's initial composition of 70%Ga<sub>2</sub>S<sub>3</sub> and 30%La<sub>2</sub>S<sub>3</sub> (% mol) was set by weighing. Materials of different colors and crystallization degrees were obtained according to the imposed technological conditions. The compound is held at the melting temperature sufficiently long to complete the components' reaction and the homogenization of the melt. Also, a definite time is needed for the melt to degas. Weight losses can occur with the process running in an open crucible. The temperature of powder mixture is slowly increased during 12 hours, after which the melt was maintained during three hour at a temperature of 1150 °C under a low pressure of Ar gas. The required quenching rate was achieved through increasing the Ar flow after switching off the RF generator. The cooling time did not exceed 5 min. In order to eliminate the gas bubbles from the melt the vacuum pump tap was opened for 15-20 s.

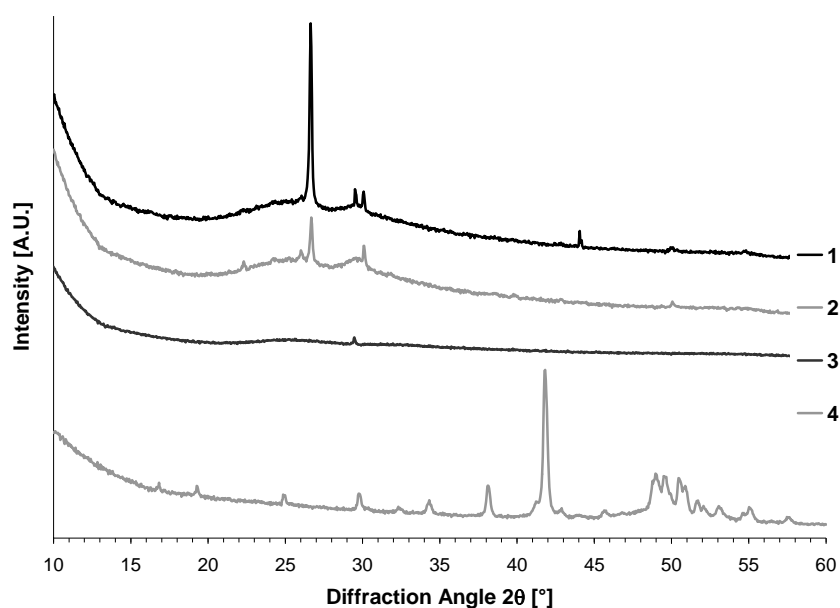


Fig.2. X-Ray Diffractograms: Pattern (1) and (2) correspond to opal sample obtained at slow quenching rate; pattern (3) corresponds to a good quality glass obtained at high quenching rate; pattern (4) corresponds to re-crystallized samples.

Initially, the material had a matt-yellowish color. Investigations by XRD (Fig. 2, patterns 1 and 2) demonstrate a considerable crystallization. To increase the quenching rate some holes were drilled at the bottom of the container, thus enhancing the direct argon gas flow. With those modifications, the obtained material was transparent and of orange-reddish color. XRD analysis (Fig. 2, pattern 3) proves an almost perfect amorphous phase. After thermal annealing for 16 hours to 620 °C, the crystallization of glass occurred. The identified main phase belongs to  $\text{Ga}_3\text{La}_{1.66}\text{S}_7$ .



*Fig.3. Images of GLS samples with the same 70%Ga<sub>2</sub>S<sub>3</sub>/30% La<sub>2</sub>S<sub>3</sub> composition. Vitreous state corresponding to quenching from 1150 °C in Argon jet (up left); Glass after polishing (down left); Foam state (up right) is obtained after heating the bulk glass up to 900 °C and quenching in Argon flow. Piece of re-crystallized at 620 °C material compared to a transparent glass before heating (down right).*

The image of the ingot is presented in Fig. 3 (up left). It was annealed to 500 °C and polished, resulting in a disc with a good optical quality (Fig. 3, down left). The disc was cut into several pieces, which were polished and further used for optical measurements. The changes occurred in the glass were investigated by AFM and optical microscopy. After re-heating at 620 °C, the glass turned into a non-transparent form of ceramics (Fig. 3, down right) that diffuses the light. Investigation through optical microscopy of this re-crystallized material demonstrates the presence of odd crystals with dimensions up to 80 μm. As AFM analysis shows, these monocrystals with relative large dimensions are inserted in a vitreous environment with nanometer roughness. The crystallization also shows up in the XRD patterns (Fig. 3, pattern 4). The comparative analysis with the database shows the  $\text{Ga}_3\text{La}_{1.66}\text{S}_7$  crystals as basic crystallization structure. The glass with this composition turns into foam at 900 °C. This form remains even after quenching at room temperature. The restoring of the vitreous form can be achieved by melting this foam at 1150 °C followed by quenching in the above-mentioned conditions.

### 3.2 Optical spectra

The material applications require homogenous highly transparent samples. The optical transmission (Fig. 4 and Fig. 5) of bulk samples shows a good transparency up to  $\lambda=10\mu\text{m}$ . The good quality of films is proved by their transmission (Fig. 6, curve 2) in the interference maxima (560 and 1090nm), which is very close to the transmission of pure BK7 (Fig. 6, curve 1) film's substrate. By measuring the optical transmission for two thicknesses (Fig. 4), optical losses can be calculated. The optical losses in the IR range were determined to be  $0.22\text{cm}^{-1}$ , which were produced in this range mainly by light scattering.

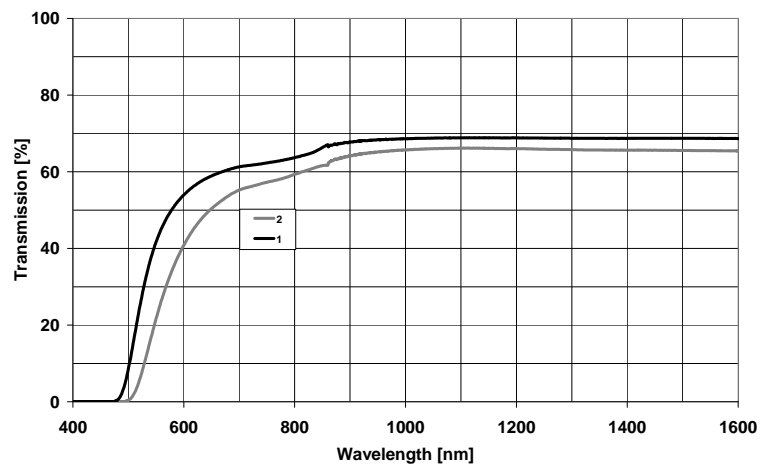


Fig.4. Optical transmission spectra of bulk GLS samples with two different thicknesses: 1.62 mm (1) and 4.10 mm (2)

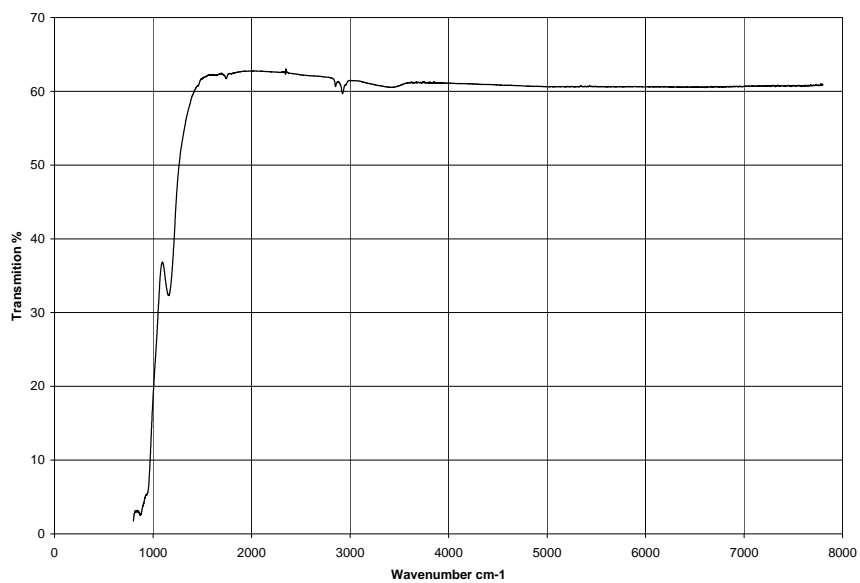


Fig.5. IR transmission spectrum of bulk GLS.

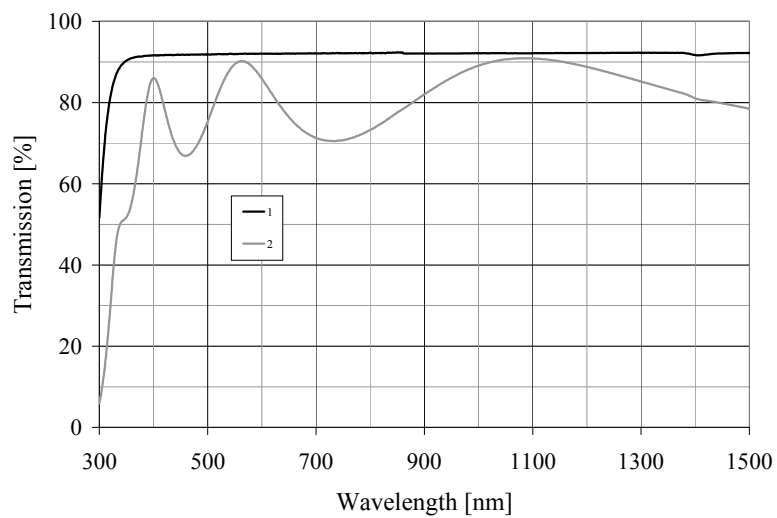


Fig.6. Optical transmission spectra of thin GLS films (2) on BK7 substrate compared to pure substrate (1).

#### 4. Discussion

Only few research groups possess the fabrication technology of high optical quality GLS glasses. This situation leads to the assumption that the technology may not be so simple. RF inductor heating used by us gives some advantages. The electric conductivity increases in semiconductor materials at high temperature, leading to the possibility of direct energy absorption provided by RF inductor and consequently to the intensive melts mixing due to convection. This may be confirmed by our experiment, where high quality glasses were obtained without any mechanical stirring. The effect of convection will be greater for a larger amount of material.

The refractive index of the films was calculated from the graph of Fig. 4 by two methods:

a) By using measurements of film thickness with a profilometer: The position of the transmission maximum was established from measured optical spectra. As thin films have the refractive index greater than that of the substrate, the refractive index determined from the condition  $n = \lambda_m / 2d$  was used, getting  $n = 2,48$ . The position of the transmission maximum  $\lambda_m$  was established from measured optical spectra. This method requires the interference order number to be known.

b) Without thickness measurements. The formula for refractive index calculation of the films was deduced [14] by using simple interference considerations. As compared to well-known results [15], the developed expression for refractive index contains (+/-) sign having physical sense for both for plus and minus:

$$n_f = \sqrt{N \pm \sqrt{N^2 - n_s^2}} \quad (1)$$

where

$$N = \frac{2n_s}{T_1} - \frac{n_s^2 + 1}{2} \quad (2)$$

The sign “+” must be used when the refractive index of the film is higher than the refractive index of the substrate, while  $T_1$  represents a minimum in the transmission spectrum. However, when the refractive index of the film is lower than the refractive index of the substrate, the sign “-” applies while  $T_1$  corresponds to maxima in transmission spectra.

In this equation the value of the substrate refractive index ( $n_s=1.506$ ) is well known as BK7 glass substrate was used. If unknown, it may be calculated from the relation:

$$n_s = \frac{1 + \sqrt{1 - T_0^{*2}}}{T_0^*} \quad (3)$$

where  $T_0^*$  is the maxima (as  $n_f \geq n_s$ ) in film transmission spectra.  $T_0^*$  changes due to substrate refractive index dispersion. In any case the measurements must be performed still far away from the fundamental absorption. The value of 2.46 for the film refractive index obtained by this method is very close to the value of 2.48 obtained earlier.

From the optical transmission of the bulk samples (Fig. 4), the refractive index of the material in the transparency band can be calculated using optical transmission formula from multiple intensity reflections:  $T = 2n/(n^2 + 1)$ , where  $T$  is the optical transmission for wavelengths far away from the fundamental absorption. We have the refractive index  $N = 2.55$  for bulk samples. It is a little greater than  $n = 2,48$  - the refractive index of thin films.

The absorption coefficient  $\alpha(\lambda)$  was calculated from the optical transmission data:

$$T(\lambda) = (1-R)^2 \exp(-\alpha d) \quad (4)$$

Using the values of the optical transmission for two thicknesses, we can exclude the unknown reflection coefficient  $R$  and calculate the absorption coefficient:

$$\alpha(\lambda) = (\ln T_1 - \ln T_2) / (d_2 - d_1) \quad (5)$$

Urbach model [16] determines in amorphous materials an exponential dependence for the localized energy states;  $\alpha(\lambda) \sim \exp(h\nu/E_u)$ .  $E_u$  represents the Urbach energy that determines how deep the energy levels extend in the band gap. According to this model, a linear dependence must exist in  $(\ln \alpha)$  and  $(h\nu/E_u)$  coordinates.  $E=h\nu$  represents the photon energy calculated as  $E [\text{eV}] = 1.24/\lambda [\mu\text{m}]$ . Calculations are presented in Fig. 7 (curve 1).

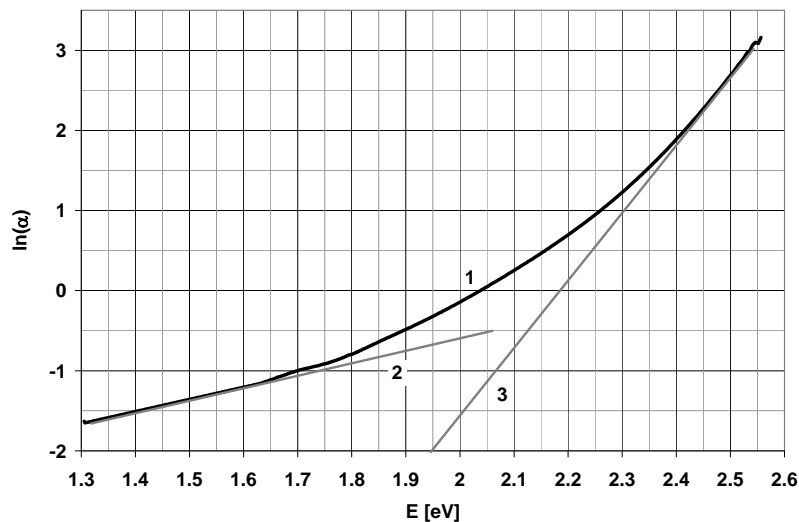


Fig.7. Processing of optical measurements: The logarithm of absorption coefficient ( $\text{cm}^{-1}$ ) versus energy of photons. Slope of the curves (1) denotes the activation energy corresponding to Urbach density of state and slope of curve (2) denotes the density of deep defect states.

The tangent of the tilt angle represents the inverse value of the activation energy. As it can be seen in this graph, two values of the activation energy may be outlined: 0.12 eV for high photon energies corresponding to Urbach tails and 0.66 eV for low photon energies, corresponding to the localized energetic levels placed deep in the band gap. There is a slow passage from one dependence to another. The energetic levels close to the band edge occur due to the potential fluctuations and they are characteristic for all amorphous materials. The energetic levels deeply extended in the band gap represent localized levels. These levels occur due to the defects and impurities in the material.

The control of the concentration of these levels has a high practical importance. In amorphous silicon, for instance, the deep energetic levels are compensated by hydrogenation of the material. Thus the amorphous silicon becomes an intrinsic semiconductor, enabling the change of the p-type electrical conductivity into n-type. The elimination of the deep energetic states is necessary in optical fibers for to diminish the optical losses. However, this effect is not always undesired. Populating of in-band energy levels with photo-electrons leads to the modification of the optical transmission. This situation can be used to achieve optical modulators in waveguides [17].

## 5. Conclusions

A new method that uses the material heating and melting by the use of energy provided by RF (radio-frequency) inductor was investigated. The direct electromagnetic field energy absorption by material gives the possibility of intensive melt mixing due to the convection phenomenon and the possibility of high quality glass preparation without any mechanical stirring. Sufficiently high quenching rate of the melted material was done by argon gas flow without taking out the crucible. Synthesis of good quality vitreous material of the composition  $70\text{Ga}_2\text{S}_330\text{La}_2\text{S}_3$  was demonstrated by XRD and by optical transmission measurements. The measured refractive

index of the glass material 2.48 for film and 2.55 for bulk is sufficiently high for the design of full gap photonic crystals. Optical losses in the proximity of IR region are quite small, of  $0.22 \text{ cm}^{-1}$ . Two kinds of exponential state distribution were established: weak states with activation energy 0.12 eV and deep states with activation energy of 0.66 eV. The main crystals that occur upon reheating the material up to a temperature higher than the glass transition have the  $\text{Ga}_3\text{La}_{1.66}\text{S}_7$  structure.

### Acknowledgements

The financial support is offered by the Ministry of Education, Research and Youth of Romania in the frame of the 27N Contract – Core Program OPRONICA III.

### References

- [1] A.M. Lozac'h, S. Banner, M. Guittard, P. Besancon, J. Flahut, *Ann. Chim.* **9**, 127 (1974)
- [2] A. Zakery, S.R. Elliott, *J. Non-Cryst. Solids*, **330**, 1 (2003)
- [3] Ruihua Li, Angela B. Seddon, *J. Non-Cryst. Solids*, **256-257**, 17 (1999)
- [4] T. Schweizer, D.J. Brady, D.W. Hewak, *OPTICS EXPRESS*, **1**, 10 (1997)
- [5] J. D. Shephard, R. I. Kangley, R. J. Hand, D. Furniss, M. O'Donnell, C. A. Miller and A. B. Seddon, *J. Non-Cryst. Solids*, **326-327**, 439 (2003)
- [6] Kimmo Paivasaari, Victor K. Tikhomirov, Jari Turunen, *OPTICS EXPRESS*, **15**, 2336 (2007)
- [7] A. Zakery, S.R. Elliott, *J. Non-Cryst. Solids*, **330**, 1 (2003)
- [8] A. Feigel, M. Veinger, B. Sfez, A. Arsh, M. Klebanov, and V. Lyubin, *App. Phys. Lett.*, **83**, 4480 (2003)
- [9] Nemeč P., Nazabal V., Pavlista M., Moreac A., Frumar M., *Mat. Chem. and Phys.*, **117**, 23 (2009)
- [10] A.K.Mairaj, P. Hua, H.N. Rutt, D.W.Hewak, *J.Lightwave Technol.*, **20**, 1578 (2002)
- [11] A.M. Andriesh, M. Bertolotti, A.Ferrari, A.A. Popescu, *J. Appl. Phys.*, **67**, 7536 (1990)
- [12] A. Popescu, S. Miclos, D. Savastru, R. Savastru, M. Ciobanu, M. Popescu, A. Lorinczi, F. Sava, A. Velea, F.Jipa, M. Zamfirescu, *J. Optoelectron. Adv. Mater.*, **11**(11), 1874 (2009)
- [13] M. Popescu, A. Velea, A. Lorinczi, M. Zamfirescu, F. Jipa, S. Miclos, A. Popescu, D. Savastru, *Dig.J.Nanomater.BIOS.*, **5**(4), 1579 (2010)
- [14] A. Popescu, D. Savastru, S. Miclos, *J. Optoelectron. Adv. Mater.*, **12**, 1012 (2010)
- [15] R. Swanepoel, *J. Phps. E: Sci. Instrum.*, **16**, 1214 (1983)
- [16] F. Urbach, *Phys. Rev.*, **92**, 1324 (1953)
- [17] A. Andriesh, O. Bolshakov, V. Zhitar, A. Popescu, *J. Non-Cryst. Solids*, **90**, 565 (1987)